

SIMS ionization of hydrogen in silicates: a case study of kornerpine†

Luisa Ottolini^a and Frank C. Hawthorne^b

^aCNR-Centro di Studio per la Cristallochimica e la Cristallografia, Via Ferrata, 1, I-27100 Pavia, Italy

^bDepartment of Geological Sciences, University of Manitoba, Winnipeg, Manitoba, Canada R3T 2N2

Received 28th June 2001, Accepted 7th September 2001

First published as an Advance Article on the web 19th October 2001

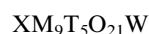
H/Si ionization in kornerpine, an (Mg, Al)-rich silicate mineral, has been investigated. There are significant variations (about 30% rel.) in the relative-to-Si ion yield for H [IY(H/Si)] as a function of chemical composition of the matrix kornerpine: ~38–45 wt% Al₂O₃, ~29–32 wt% SiO₂, ~15–20 wt% MgO, ~0–11 wt% FeO_{tot}, ~2–4 wt% B₂O₃ and minor variations for the remaining components. There are strong correlations between IY(H/Si) and (Fe + Mn)(at) [where (at) represents the cation abundance in the sample (by atoms)] ($r^2=0.80$); for Mg and Al(at), $r^2=0.73$ and 0.90 , respectively. The absolute ion yield for H [IY(H)] is strongly correlated with (Fe + Mn)- and Si(at) ($r^2=0.92$ and 0.94 , respectively). It is possible to make adequate corrections to IY(H/Si) as a function of sample composition to obtain accurate H₂O (wt%) concentrations, reducing (if not overcoming) the need for specific standards (in most cases unavailable) that match the chemical composition of the sample. A model is proposed for H ionization in this matrix. The present outcome is qualitatively similar to the results obtained for other silicates (schorl, foidite, dravite, axinite, amphibole) and represents a valid basis for modelling SIMS ionization of H in silicates.

Aim of investigation

In SIMS analysis of H in silicates, when H is present as a minor constituent, matrix effects are a major limitation in the quantification of H⁺ signal intensity as wt% concentration of H₂O (Ottolini *et al.*¹ and references therein). Secondary-ion intensity can be non-linearly related to element concentration, but it depends to various extents on the concentration of other element(s) in the matrix, on the chemical character of the primary ions used, on chemical bonding and structure of the matrix and, in some cases, on the crystallographic orientation of the primary beam relative to the sample surface.² Previous investigations of H in several minerals have shown that matrix effects, if well calibrated, allow high levels of accuracy to be achieved (range: 5–10% rel.) (*e.g.*, Andreozzi *et al.*³). However, in the absence of suitable standards, quantification may be inaccurate if proper matrix corrections are not applied. A set of well-characterized kornerpines^{4,5} was used in the present SIMS study to investigate chemical matrix effects affecting H ionization during analysis with the ion microprobe.

Kornerpine

The chemical composition of kornerpine may be written as:



where

X = □, Mg, Fe²⁺

M = Al, Mg, Fe²⁺, Fe³⁺, (V³⁺, Cr³⁺, Ti⁴⁺)

T = Si, B, Al

W = OH, F

Details about the structure can be found in refs. 4 and 5.

The mineral has a reasonable range in matrix chemistry but

has a relatively restricted variation in H content. The composition of the samples investigated here is reported in Table 1. The Fe²⁺/Fe³⁺ ratios were calculated such that the relationship for mean bondlength *versus* aggregate radii of the constituent cations is linear for the complete sample set of kornerpine crystal structures. In this set of kornerpine, H is about 1 wt% (as H₂O) and the other oxides vary in the following range: ~38–45 wt% Al₂O₃, ~29–32 wt% SiO₂, ~15–20 wt% MgO, ~0–11 wt% FeO_{tot}, ~2–4 wt% B₂O₃, 0–0.31 wt% MnO and minor variations for the remaining cations. The W site in the formula is occupied by both (OH) and F, and it has been shown that OH + F = 1.00 apfu (atoms per formula unit).⁵ Hydrogen contents were measured by hydrogen-line extraction. The sample was heated at 1400 °C inside a quartz extraction vessel and the resultant gases were collected in a trap held at −196 °C. The accumulated H₂O was separated from any other gases by differential freezing, and then reacted with U at 750 °C to produce H₂ which was collected on charcoal at −196 °C and measured manometrically. Full details are given by Kyser and O'Neil.⁶ The resulting values are equal to the amount of H₂O required for the relation (OH + F) = 1.0 atoms per formula unit, and this result is in accord with the crystal-structure results. Hence this relation was used to derive the H₂O content for all kornerpine samples.

Experimental strategy

In silicates, Si is commonly selected as the inner reference element in SIMS quantification procedures. For this reason, our interest was: (1) to assess all matrix effects affecting the relative-to-Si ion yield for H, IY(H/Si) = [H⁺/Si⁺]/[H(at)/Si(at)], where H⁺ and Si⁺ represent the secondary ion signals, and (at) the cation abundance (by atoms); (2) to uncouple matrix effects affecting the ionization of H⁺ from those affecting the ionization of Si⁺ secondary ions; and (3) to combine SIMS experimental data with information on crystal

†Presented at the XVI International Conference on X-ray Optics and Microanalysis (ICXOM), Vienna, Austria, July 2–6, 2001.

Table 1 Reference composition⁴ of the kornerupine crystals used in the present study (average of 10 points); blank entries are values near the detection limit and <0.01 apfu

	K2	K9	K10	K15	K17	K22	K23	K32	K8	K25
SiO ₂	30.75	30.89	29.96	29.69	29.86	30.84	31.63	30.69	29.01	30.07
TiO ₂			0.13	0.15			0.16			0.19
Al ₂ O ₃	42.98	40.11	40.36	37.75	38.57	44.76	42.63	40.66	41.36	38.79
B ₂ O ₃ ^a	2.41	3.96	3.22	3.24	3.52	1.99	3.49	3.80	2.51	3.90
Fe ₂ O ₃ ^b	0.86	0.60	1.52	3.63	3.44	0.09	—	0.17	2.21	2.19
FeO	2.25	4.26	7.62	7.25	7.34	1.21	—	2.48	7.41	7.96
MnO	—	0.13	—	—	—	—	0.15	—	0.31	—
MgO	18.79	18.05	15.15	16.03	15.24	19.35	19.91	19.45	15.03	14.91
V ₂ O ₃	—	—	—	—	—	—	0.20	—	—	—
Na ₂ O	—	0.05	—	0.11	0.12	—	—	—	—	0.06
H ₂ O ^c	1.20	1.03	1.14	0.95	1.01	1.23	1.19	1.14	1.17	0.83
F	0.04	0.38	0.11	0.49	0.37	—	0.10	0.15	0.02	0.75
O=F	−0.02	−0.16	−0.05	−0.21	−0.16	−0	−0.04	−0.06	−0.01	−0.32
Total	99.26	99.31	99.15	99.08	99.31	99.46	99.42	98.48	99.03	99.34
Si	3.787	3.811	3.779	3.779	3.779	3.769	3.822	3.784	3.690	3.792
Al	0.701	0.345	0.521	0.509	0.453	0.811	0.450	0.408	0.758	0.360
B	0.512	0.844	0.700	0.712	0.768	0.420	0.728	0.808	0.552	0.848
ΣTet.	5.000	5.000	5.000	5.000	5.000	5.000	5.000	5.000	5.000	5.000
Al	5.537	5.487	5.479	5.154	5.300	5.636	5.620	5.501	5.443	5.405
Mg	3.450	3.320	2.849	3.042	2.876	3.525	3.586	3.576	2.850	2.803
Fe ²⁺	0.396	0.440	0.804	0.772	0.777	0.124	—	0.256	0.788	0.839
Fe ³⁺	0.080	0.056	0.144	0.348	0.328	0.008	—	0.016	0.212	0.208
Mn ²⁺	—	0.014	—	—	—	—	0.015	—	0.033	—
V ³⁺	—	—	—	—	—	—	0.019	—	—	—
Cr ³⁺	—	—	—	—	—	—	—	—	—	—
Ti	—	—	0.012	0.014	—	—	0.015	—	—	0.018
Na	—	0.012	—	0.027	0.029	—	—	—	—	0.015
Ca	—	—	—	—	—	—	—	—	—	—
CATSUM	14.298	14.329	14.287	14.358	14.311	14.293	14.255	14.349	14.327	14.287
F	0.016	0.148	0.044	0.197	0.148	0.000	0.038	0.058	0.008	0.299
OH	0.984	0.852	0.956	0.803	0.852	1.000	0.962	0.942	0.992	0.701

^aB via SREF at T(3). ^bFe³⁺ via SREF at M(4). ^cAnion normalization based on O₂₁ (OH + F)₁.

structure and chemical composition, and propose a model for the ionization of H in this sample set.

Description of the experimental procedures

Of the kornerupine samples available,^{4,5} we have considered the following as inner standards: K2, K9, K10, K15, K17, K22, K23 and K32. Crystals K8 and K25 were used as test samples for the analytical procedure. Samples were analyzed with a Cameca IMS 4f ion-microprobe (installed at CNR-CSCC, Pavia) with a 12.5 kV accelerated ¹⁶O[−] primary-ion beam of 5 nA current intensity and Ø equal to about 10 µm. Secondary ions of H⁺ and ³⁰Si⁺ of about 75–125 eV (Ottolini *et al.*¹) were monitored with an ion image field of 25 µm (400 µm contrast diaphragm and 1800 µm field aperture). Acquisition times were 30 s for H and Si each, over 10 cycles. Steady-state sputtering was achieved after 600 s. The duration of a complete analysis was 20 min. All samples were analyzed two or three times within a one-day analytical session (12 h) to minimize any variation in experimental conditions. Ionization of H/Si is significantly affected by the primary-beam density that, in turn, is dependent on the ion-beam focusing conditions, on the “age” of the electrodes of the primary-ion source (duoplasmatron), and on other experimental factors that can change slightly from day-to-day.

In the calculation of the IY(H/Si), the reference H₂O (wt%) value used was that derived from stoichiometry,^{4,5} and, for SiO₂ (wt%), that derived by electron-microprobe analysis (Table 1).

Results

Relative-to-Si ion yield for H

Table 2 reports the linear-fit equations of the experimental ion yields, IY(H/Si), as a function of the cation abundance (at) by

atoms of the matrix constituents, together with the *r*² values. Deloule *et al.*⁷ investigated possible relationships between instrumental mass fractionation and elemental emissivity in amphiboles. Matrix effects on instrumental D/H fractionation were calibrated empirically as a function of the beam intensity of major chemical species. The best fit was obtained by means of a linear combination of secondary-ion intensities *I_j* (where *j* represents the element *j* corrected for isotopic abundances), normalized to a unit sum over all measured elements. Havette and Slodgian⁸ expressed the relative-to-Si ion yield of an element (X) in silicates, *R*_{Si}^X, as:

$$R_{Si}^X \approx K_{Si}^X [Si] + K_{Si}^X [Al] \dots$$

where *K*_{Si}^X represents the relative ionization yield of element X in a silica matrix, and [Si] and [Al] represent the cationic concentrations of Si and Al in the mineral. A calibration

Table 2 Linear fit of experimental IY(H/Si), IY(H), IY(Si) values (indicated as *y*) vs. matrix-cation abundances (at) (by atoms), indicated as *x*, and relative regression index (*r*²) in the set of kornerupine samples studied in the present work

Ion yield	(at)	Regression line	<i>r</i> ² coefficient
IY(H/Si)	(Fe + Mn)	<i>y</i> = 0.183 − 0.369 <i>x</i>	0.80
	(Fe + Mn + Ti + V)	<i>y</i> = 0.183 − 0.372 <i>x</i>	0.80
	Mg	<i>y</i> = 0.418 <i>x</i> − 0.029	0.73
IY(H)	Mg	Slope > 0	0.86
	Si	Slope > 0	0.94
	(Fe + Mn)	Slope < 0	0.92
	(Fe + Mn + Ti + V)	Slope < 0	0.90
IY(Si)	(Fe + Mn)	Slope > 0	0.56
	Si	Slope < 0	0.28
	Mg	Slope < 0	0.50

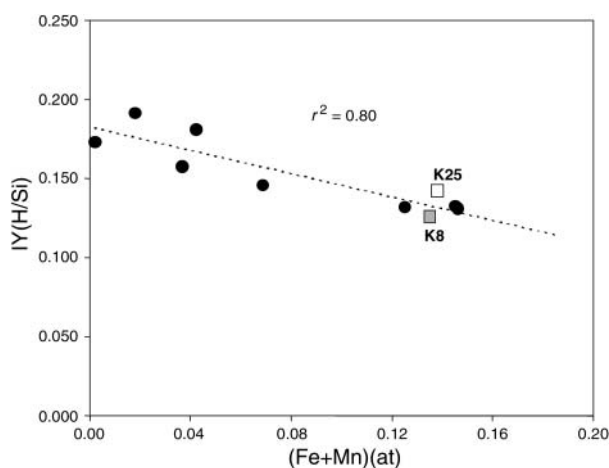


Fig. 1 Regression line of the relative-to-Si ion yield for H; $IY(H/Si)$ [$H^+/H(at)/Si^+/Si(at)$] vs. $(Fe+Mn)(at)$ [where (at) represents the cation abundance (by atoms)] for the crystals investigated in the present study. K8 and K25 are the test samples. Their IY are reported for comparison.

procedure with 25 known standards has been used for determining the relative ionization coefficients involved in this linear relation.

In our samples, Fe is the most abundant transition element whose concentration varies significantly in the sample set. Mn, V and Ti contents are low or null in all crystals (Table 1). The experimental data (Fig. 1) are rather scattered at concentrations of matrix components below 0.12 (at). With increasing transition-element concentration, $IY(H/Si)$ decreases linearly, varying from about 0.19 to 0.125, for a variation in $(Fe+Mn)(at)$ of about 0 to 0.15. Experimental IY data for test samples K8 and K25 are also shown in Fig. 1, the higher value pertaining to K25. A similar equation and r^2 value ($=0.80$) were obtained for $IY(H/Si)$ vs. $(Fe+Mn+Ti+V)(at)$. The correlation index r^2 for $IY(H/Si)$ vs. $Mg(at)$ is lower (Table 2), the data being rather scattered for $x > 0.45(at)$ (Fig. 2); for $IY(H/Si)$ vs. Al, it is higher ($r^2=0.90$). Al is the most abundant matrix cation (38–45 wt% Al_2O_3 in the sample set) and correlates with changes in Fe and Mg content in the matrix. $IY(H/Si)$ increases with increasing Si content in the matrix. Also, in this case, the experimental data are rather scattered ($r^2=0.56$). The correlation improves for $IY(H/Si)$ vs. $(Al+Si+Mg+Na+Fe+Mn+Ti+V)(at)$ in the matrix ($r^2=0.98$)

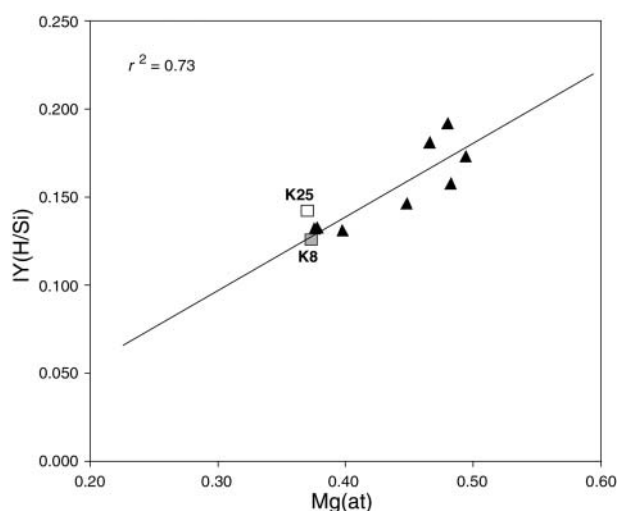


Fig. 2 Regression line of $IY(H/Si)$ vs. $Mg(at)$ for the reference crystals. The test samples K8 and K25 are reported for comparison. The data are rather scattered for Mg content $> 0.45(at)$.

and worsens if the sum also includes B and B plus H ($r^2=0.71$ and 0.79, respectively).

$IY(H/Si)$ is thus a complex function of the chemical composition of the matrix. It increases with increasing major element (at) contents. The higher value (0.192) is for K22, which has the maximum concentration of $(Al+Si+Mg)$ in the sample set ($=1.87 at$). High values for $IY(H/Si)$ are also characteristic of K2 [$(Al+Si+Mg)(at)=1.82$; $IY(H/Si)=0.181$], and sample K23 [$(Al+Si+Mg)(at)=1.86$; $IY(H/Si)=0.173$].

Absolute ion-yields for H and Si

As the relative-to-Si ion yield for H is defined by the ratio of two ratios (intensity to concentration for H, normalised to that of Si), it is useful to uncouple the ionization behaviour of H from that of Si, and to investigate separately the absolute ion yields [i.e., $IY(H)=H^+/H(at)$ and $IY(Si)=Si^+/Si(at)$] as a function of matrix composition. Small fluctuations in ion current or variation in focusing conditions have a direct effect on the absolute ion yield. Moreover, the primary-beam current intensity cannot be monitored during ion bombardment. For this reason, Si is conventionally used as the inner reference during SIMS analysis in silicate matrices. Any fluctuation in H^+ ion signal is reduced (if not eliminated) when normalising the H^+ ion signal to the Si^+ ion signal. In the present study, the $^{16}O^-$ intensity of the primary beam was reasonably stable during analysis. Nevertheless, when necessary, it was re-adjusted to 5 nA and the ion beam was re-focussed before starting a new analytical run.

With this in mind, we have normalised the experimental H^+ secondary-ion intensities to $H(at)$ for each sample, and plotted the resulting absolute ion yields for H as a function of major-element concentrations in the standards. $IY(H)$ increases linearly with increasing Mg ($r^2=0.86$; Fig. 3) in the matrix. There is a strong correlation ($r^2=0.94$) for $H^+/H(at)$ vs. $Si(at)$ (Fig. 4). The absolute ion yield for H increases with increasing Si [range about 0.495–0.53 $Si(at)$] and decreases with increasing $(Fe+Mn)$ contents (Fig. 5); the r^2 value of 0.92 is comparable to the one above.

$Si^+/Si(at)$ increases linearly with increasing transition-metal content (Fig. 6), although the correlation index is not high ($r^2=0.56$). The variation in the inverse function, $Si(at)/Si^+$ vs. transition elements in the matrix, is comparable to that of the absolute H ion yield, shown in Fig. 5 (about 17% rel.). $IY(H/Si)$ can be written as $IY(H/Si)=[H^+/H(at)] \times [Si(at)/Si^+]$. When combining the absolute ion yields (for H and Si) vs. $(Fe+Mn)(at)$, the overall variation is about 30% (Fig. 1). Thus the

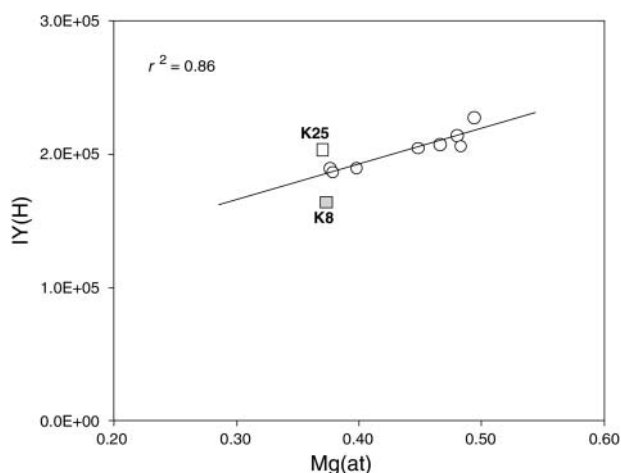


Fig. 3 Regression line of the absolute ion yield for H; $IY(H)$ [$H^+/H(at)$] vs. $Mg(at)$ for the reference crystals. K8 and K25 show, respectively, a slightly lower and higher IY than that predicted by the linear fit.

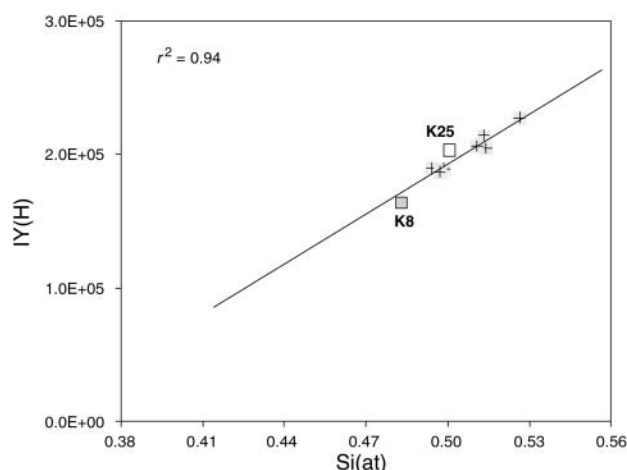


Fig. 4 Regression line of IY(H) vs. Si(at) for the crystals investigated in the present study (standards and test samples K8 and K25). The data are well correlated and show a clear increase of the IY(H) with increasing Si content in the matrix.

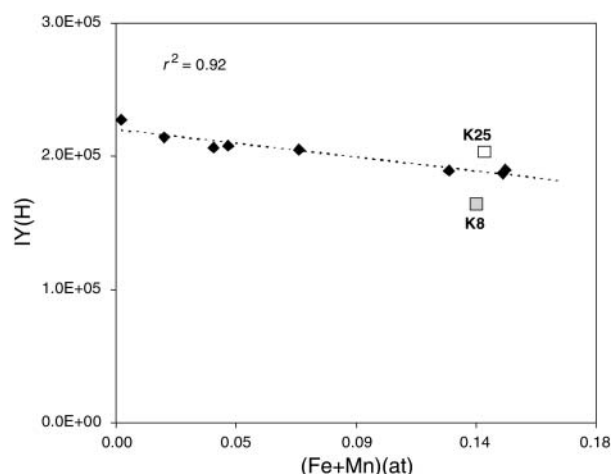


Fig. 5 Regression line of IY(H) vs. (Fe+Mn)(at) for the crystals of the present study. The data are well correlated for the standards and show a definite decrease of the IY(H) with increasing (Fe+Mn) content in the matrix. The test samples show a different ion yield, higher for K25 and lower for K8. See text for discussion.

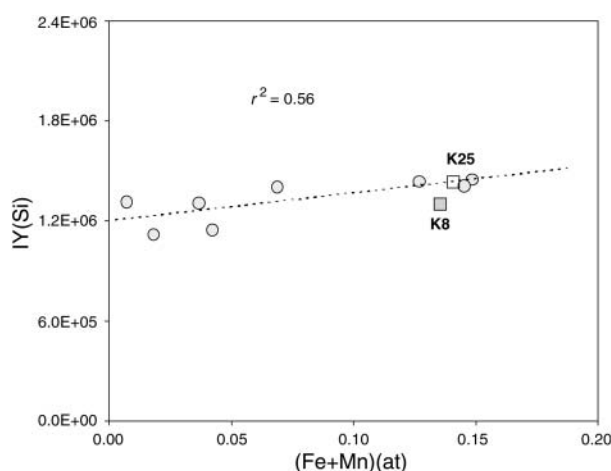


Fig. 6 Regression line of the absolute ion yield for Si; IY(Si) [Si⁺/Si(at)] vs. (Fe+Mn)(at) for the crystals investigated in the present study. IY(Si) increases slightly with increasing (Fe+Mn) content but the correlation is weak ($r^2=0.56$).

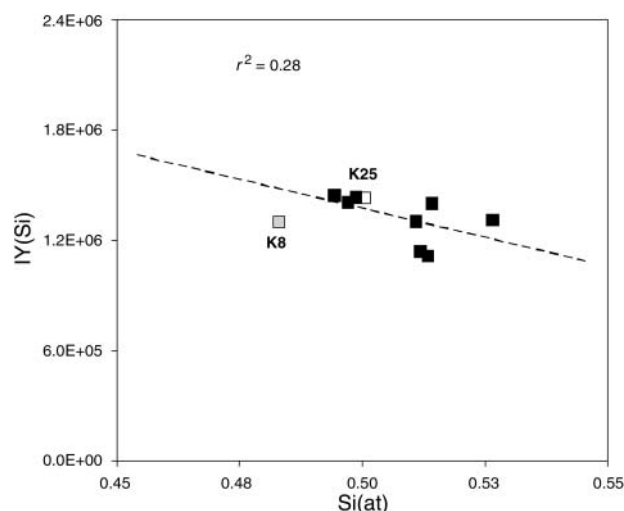


Fig. 7 Regression line of IY(Si) vs. Si(at). IY(Si) decreases with increasing Si content. The test samples K8 and K25 are reported for comparison. The data are rather scattered for all crystals ($r^2=0.28$).

total matrix effect associated with the relative-to-Si ion yield for H is equivalent to the sum of the variation of both absolute ion yields.

Si⁺/Si(at) is not significantly correlated with Si(at) ($r^2=0.28$) (Fig. 7) and Mg ($r^2=0.50$), but shows a better correlation with Al ($R^2=0.80$). In each case, IY(Si) decreases (to different extents) with increasing Al, Si and Mg contents in the matrix. There is a stronger correlation ($r^2=0.90$) between IY(Si) and (Al+Mg+Na+Fe+Mn+Ti+V)(at) in the matrix. It worsens after adding Si, Si+B, and Si+B+H ($r^2=0.82, 0.44, 0.55$, respectively).

If we use the calibration with IY(H/Si) vs. (Fe+Mn)(at) (Fig. 1) for the crystals used as standards, agreement with the reference H₂O values is in the range 2–9% rel. for all samples, the differences being mostly within the uncertainty of analysis ($\pm 3\sigma$). For the test samples (K8 and K25), the SIMS H₂O contents are 1.11 and 0.90 wt%, respectively. These samples are characterized by a quite different chemistry from other Fe-rich samples. Nevertheless, the discrepancy between SIMS values and the reference is only 8% and we can reasonably consider it within the overall analytical uncertainty [as due to both the “error” in the reference H₂O data itself and to the (EPMA+SIMS) experimental procedures].

Discussion

In our sample set, Al is the most abundant metal in the matrix. Moreover, variation of SiO₂ in the sample set is limited (29.01–31.63 wt% SiO₂) relative to that of Al₂O₃ (37.75–44.76 wt%) and MgO (15.03–19.91 wt%). Note that Al₂O₃ and MgO vary sympathetically in the sample set.

The absolute ion yield for H, IY(H), increases with increasing Al, Si and Mg contents (Table 2).

The samples with the highest Fe content [K15, K17, K8 and K25] are also those with the lowest Al and Mg contents, and, for these samples, the IY(H/Si) values are the lowest in the sample set.

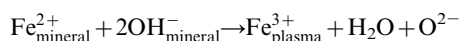
During H isotope analysis, Si and (Mn,Fe) were found to induce the strongest shifts of instrumental mass bias α_{instr} .⁷ In the present case, IY(H) is well correlated with the Fe (+Mn) and Si content of the matrix. Our results are also consistent with previous measurements that noted increased H sensitivity with SiO₂ content.⁹

In Fig. 7, we see that IY(Si) shows much more scatter than IY(H), suggesting that normalization of the H⁺ ion signal to another element of the matrix may be more appropriate. IY(Si) increases slightly with increasing (Fe+Mn). However, the

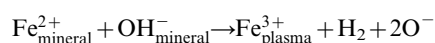
correlation is weak ($r^2=0.56$), and we suggest that Si ionization is not directly affected by the (Fe+Mn) content in the matrix, perhaps because of the relatively low amounts of transition metals (maximum about 11 wt%) relative to the SiO₂ content (about 29–32 wt%) in this sample set. The values of IY(Si) are rather scattered at low values of (Fe+Mn)(at) in the matrices (K2, K22, K23 and K32) and the correlation improves at higher (Fe+Mn) contents (K15 and K17). Ion yield (and isotope fractionation) variations are often correlated with mean atomic weight (which largely follows the variation in Fe content) or to sputter-rate effects on ionization.¹⁰ The sputter-rate differences among these samples are unknown, and thus the importance of this parameter cannot be established. The decrease of ion yield with increasing Fe (+Mn) content is also well-established, being associated with a corresponding decrease of Al in the matrix.

Experiments on minerals using a ¹⁶O[−] primary beam show that the oxides observed in the mass spectrum are not directly related to the oxide structure of the solid, but are the reaction products of ¹⁶O[−] implanted primary ions and sample atoms interacting at high temperature.¹¹ Under these circumstances, the dominant molecular species detected are monoxides that are generally stable and have a long lifetime in the sputtering region (as reflected by their high dissociation energies). Oxygen represents 50% or more of the total number of atoms in silicates; moreover, the additional oxygen, carried by the O[−] primary beam and implanted into the subsurface region of the sample, locally increases the overall oxygen budget. This large concentration of oxygen acts as a chemical buffer, enhancing the oxidation processes in the sputtering region and increasing the amount of simple metal–oxide ions relative to the fraction of complex molecular secondary ions coming from the matrix atoms (*i.e.*, Si, Al, Mg).

For H-bearing minerals, such as kornerupine, oxidation *via* dehydroxylation could occur where the ion beam impinges on the sample during sputtering/ionization:



or possibly



The temperatures involved in SIMS processes range from 5000 to 15000 K, the highest temperatures pertaining to insulators such as silicates. As pointed out by Andersen and Hinthorne¹¹ there must be a temperature gradient between the hot ion-emitting region and the cold bulk-sample. Our hypothesis is that oxidation/dehydroxylation could occur in the sample-sputtering region, causing a decrease in the IY(H/Si) with increasing Fe content of the sample, thereby promoting loss of H from the sputtering region as neutral molecules and thus reducing the number of H⁺ ions during ¹⁶O[−] bombardment.

It is very probable that Mn behaves in a similar fashion to Fe, due to their chemical affinity. Havette and Slodzian⁸ reported that Fe³⁺ seems to have a greater effect on the ionization of other elements (for instance Al) than Fe²⁺. Decrease in IY(H/Si) with increasing Fe (and Mn) content in the matrix was previously observed in silicates such as schorl and dravite,² foidite,¹² axinite³ and amphibole (CNR ion-probe unpublished results). In particular, we found³ that the sample which showed the highest matrix effects (ax 47) also had the highest Mn content (MnO=12.5 wt%) and its Fe content was present mostly as Fe³⁺. For tourmaline of schorl-elbaite composition,¹³ variation in IY(H/Si) of about ±10% rel. was detected in the samples investigated; FeO and MnO each varied in the range about 0–7 wt%. In that case, the reference H₂O (wt%) values [from which IY(H/Si) was calculated] were derived by stoichiometric arguments (samples from Burns

*et al.*¹⁴) and from thermal analysis (all other samples of the set), and the experimental data were collected in a two-month span over three analytical sessions.

Conclusions

The novel results of the present work may be summarized as follows:

(1) IY(H/Si) is positively correlated with Al, Si and Mg contents and negatively correlated with increasing transition-metal content in the matrix.

(2) There are fairly strong correlations for IY(H/Si) *vs.* (Fe+Mn)(at) ($r^2=0.80$), for IY(H/Si) *vs.* Mg(at) ($r^2=0.73$); between IY(H) and Si and (Fe+Mn)(at), $r^2=0.94$ and 0.92 , respectively.

(3) As a direct consequence of this investigation, accurate analysis is feasible for H₂O in kornerupine of any composition by using a very small number of standards. In particular, the linear equation obtained for IY(H/Si) *vs.* (Fe+Mn)(at) allows straightforward quantification of H₂O in the unknowns using only two reference kornerupine samples, preferably with high- and low-Fe contents. It is even possible to use only one standard plus a scaling factor if the experimental set-up is the same as that used here.

(4) The accuracy is estimated in the range 3–10% rel. The best value (about 3% relative) is comparable to the overall analytical precision (over a one-day span) using the present experimental set up.

(5) A model is proposed for H/Si ionization in this sample set. It takes into account the decrease of IY(H/Si) with increasing (Fe+Mn) in the matrix. It is a significant step towards modelling H/Si ionization processes in silicates.

Acknowledgements

The Consiglio Nazionale delle Ricerche (Italy) is acknowledged for financing the SIMS laboratory at CNR-CSCC (Pavia) whose facility was used in the present study. FCH was supported by grants from the Natural Sciences and Engineering Research Council of Canada. The authors wish to express their gratitude to an anonymous referee for his constructive criticism that improved the quality of this paper.

References

- 1 L. Ottoloni, P. Bottazzi, A. Zanetti and R. Vannucci, *Analyst*, 1995, **120**, 1309.
- 2 L. Ottoloni, F. Cámara, F. C. Hawthorne and J. Stirling, *Am. Mineral*, submitted for publication.
- 3 G. B. Andreozzi, L. Ottoloni, S. Lucchesi, G. Graziani and U. Russo, *Am. Mineral.*, 2000, **85**, 698.
- 4 M. A. Cooper, F. C. Hawthorne and E. S. Grew, *Can. Mineral.*, submitted for publication.
- 5 M. A. Cooper, F. C. Hawthorne, L. Ottoloni, E. S. Grew and T. K. Kyser, *Can. Mineral.*, submitted for publication.
- 6 T. K. Kyser and J. R. O'Neil, *Geochim. Cosmochim. Acta*, 1984, **48**, 2123.
- 7 E. Deloule, C. France-Lanord and F. Albarede, *The Geochemical Society, Special Publ. No. 3*, ed. H. P. Taylor, Jr., J. R. O'Neil and I. R. Kaplan, 1991, p. 53.
- 8 A. Havette and G. Slodzian, *J. Phys. Lett.*, 1980, **41**, L247.
- 9 E. Deloule, O. Paillat, M. Pichavant and B. Scaillet, *Chem. Geol.*, 1995, **125**, 19.
- 10 J. M. Eiler, C. Graham and J. W. Valley, *Chem. Geol.*, 1997, **138**, 221.
- 11 C. A. Andersen and J. R. Hinthorne, *Anal. Chem.*, 1973, **45**(8), 1421.
- 12 C. Aurisicchio, L. Ottoloni and F. Pezzotta, *Eur. J. Mineral.*, 1999, **11**, 217.
- 13 L. Ottoloni and F. C. Hawthorne, *Eur. J. Mineral.*, 1999, **11**, 679.
- 14 P. C. Burns, D. J. MacDonald and F. C. Hawthorne, *Can. Mineral.*, 1994, **32**, 31.